



Transport properties of ultra-thin granular $\text{YBa}_2\text{Cu}_3\text{O}_{7-\delta}$ nanobridges



E. Bar^a, D. Levi^a, G. Koren^b, A. Shaulov^a, Y. Yeshurun^{a,*}

^a Department of Physics, Institute of Superconductivity and Institute of Nanotechnology and Advanced Materials, Bar-Ilan University, Ramat-Gan 52900, Israel

^b Department of Physics, Technion – Israel Institute of Technology, Haifa 32000, Israel

ARTICLE INFO

Article history:

Received 6 February 2014

Received in revised form 23 March 2014

Accepted 25 March 2014

Available online 12 April 2014

Keywords:

High-temperature superconductors

Nano-wires

Magnetoresistance oscillation

Negative magnetoresistance

Negative magnetoresistance slope

Hot spots

ABSTRACT

Magneto-transport measurements in $\text{YBa}_2\text{Cu}_3\text{O}_7$ nanobridges, patterned on laser ablated ultra-thin films, reveal phenomena that are usually absent in the bulk of the material. These include broadening of the resistive transition, magnetoresistance oscillation, negative magnetoresistance at low fields, negative magnetoresistance slope at high fields, and V - I curves that exhibit voltage jumps at temperatures well below T_c . These phenomena, attributed to the granular nature of the bridges, should be taken into account in any future attempts to utilize such bridges in technological applications.

© 2014 Elsevier B.V. All rights reserved.

1. Introduction

The impressive progress in nano fabrication techniques has made it possible to realize nanobridges of various superconducting materials. Investigation of the magneto-transport properties of such bridges is a subject of both applied and fundamental research. The applied research is motivated by a desire to apply superconducting nanobridges in future electronic circuits and devices [1]. For example, superconducting nanowires may serve as interconnects in future energy efficient large computing systems. The fundamental studies deal with effects such as thermally-activated and quantum phase slips which give rise to resistance below T_c [2]. Since the discovery of high- T_c superconductors (HTS), attention has been drawn to nanobridges and nanowires made of e.g. $\text{Bi}_2\text{Sr}_2\text{CaCu}_2\text{O}_{8+x}$ (BSCCO) [3,4], $\text{Nd}_{1.2}\text{Ba}_{1.8}\text{Cu}_3\text{O}_z$ (NBCO) [5], and $\text{La}_{1.85}\text{Sr}_{0.15}\text{CuO}_4$ (LSCO) [6,7]. Special attention was devoted to $\text{YBa}_2\text{Cu}_3\text{O}_{7-\delta}$ (YBCO) [8–15] probably because of its relatively high critical temperature and high critical current. These studies revealed many interesting phenomena. For example, Arpaia et al. [15] obtained YBCO nanowires with cross-sections of $50 \times 50 \text{ nm}^2$ with critical current densities up to 10^8 A/cm^2 at 4.2 K, approaching the theoretical depairing current limit. Bonetti et al. [13] reported on telegraphic like fluctuations in the resistance of under-doped YBCO wires of width down to 100 nm, at

temperatures between the pseudo-gap temperature T^* and the superconducting transition temperature T_c . Mikheenko et al. [14] reported on YBCO wires with widths down to 50 nm that showed suppression of superconductivity when the room temperature resistance was greater than the superconducting resistance quantum, $R_q = h/4e^2$. Xu and Heath [10] succeeded in fabricating YBCO wires with width as small as 10 nm and observed transition broadening due to thermally activated phase slips, with negligible effect of external magnetic field up to 5 T.

In this paper we review our magneto-transport measurements in granular, ultra-thin YBCO nanobridges [16,17]. The phenomena observed in such bridges include systematic broadening of the resistive transition with decreasing the cross sectional area of the bridges, magnetoresistance oscillations, negative magnetoresistance at low fields and negative magnetoresistance slope in the Tesla regime. In reviewing these phenomena we add more data and, in addition, we describe new measurements of the voltage-current (V - I) characteristics in YBCO nanobridges. These V - I curves exhibit behavior characteristic of an array of Josephson junctions, unlike the behavior observed in homogeneous bridges of another HTS system [18]. In addition, some of our YBCO bridges exhibit voltage jumps at temperatures well below T_c . All these phenomena are ascribed to the granular nature of our bridges.

2. Experimental

Pulsed Laser Deposition technique was used to grow 10–20 nm thick optimally doped, epitaxial YBCO films on $10 \times 10 \text{ mm}^2$ (100)

* Corresponding author. Tel.: +972 544810575.

E-mail addresses: yeshurun@mail.biu.ac.il, yosiyeshurun@gmail.com (Y. Yeshurun).

SrTiO₃ wafers. The growth conditions are described in Ref. [19]. This technique resulted in granular YBCO films with grain sizes typically between 50 and 100 nm. AFM measurements show that more than 95% of the grains are *c*-axis oriented (the *a*-axis grains are taller than the *c*-axis grains that have 2D screw dislocation growth mode) and that the grain boundary angles are 2–3° at most.

The films were spin-coated with poly(methyl methacrylate) (PMMA) electron-beam resist, and subsequently baked for 90 s on a hotplate at 180 °C. After coating the positive PMMA on top of the YBCO film, the film was exposed in pattern shown in Fig. 1 (blue frame) to define a 700 nm long and 80–500 nm wide bridges, including the contact-pads for the four-probe measurements, using a CRESTEC CABLE-9000C high-resolution electron-beam lithography system. The exposed PMMA was removed so that only the pads and the wire remain with PMMA protection. The unprotected film areas can be removed by standard ion milling etch process. A Quantum Design Physical Properties Measurements System PPMS-6000 was exploited to measure the bridge resistance in the temperature range between 10 and 300 K and magnetic fields up to 5 T, using DC bias currents between 250 nA and 20 μA. The magnetic field was applied normal to the film surface (parallel to the crystallographic *c*-axis).

3. Results and discussion

3.1. Resistive transition

Fig. 2 shows the temperature dependence of the zero-field resistance of a set of YBCO bridges with width 80, 160, 200 and 500 nm patterned on a 10 nm thick film, measured with bias current of 5 μA. The onset of superconductivity is at approximately 88 K for all wires, reflecting the transition to a superconducting state in the grains. The figure shows a clear transition broadening as the wire width decreases. The transition width, defined as the width of the dR/dT peak at half maximum, increases as the wire width decreases, as shown in the inset to Fig. 2. For this particular set of samples, the transition width, increases from 2 K to 7 K as the bridge width narrows down from 500 to 80 nm. In homogeneous bridges, broadening of the resistive transition is observed in bridges with dimensions comparable to the coherence length and attributed to thermally activated phase slips. Clearly, in granular samples phase fluctuations at weak links play a dominant role and the broadening can be observed in bridges with dimensions much larger than the coherence length. In such bridges, as temperature is reduced the probability for current-flow channels with relatively strong links is increased and hence the effect of fluctuations

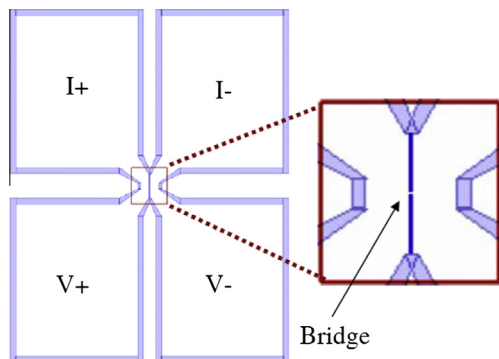


Fig. 1. YBCO bridge and pads pattern. The blue color indicates the exposed areas which were removed after ion milling. The residue (white) shows the 4-pads connected to the bridge. The right panel zooms on the bridge area. (For interpretation of the references to colour in this figure legend, the reader is referred to the web version of this article.)

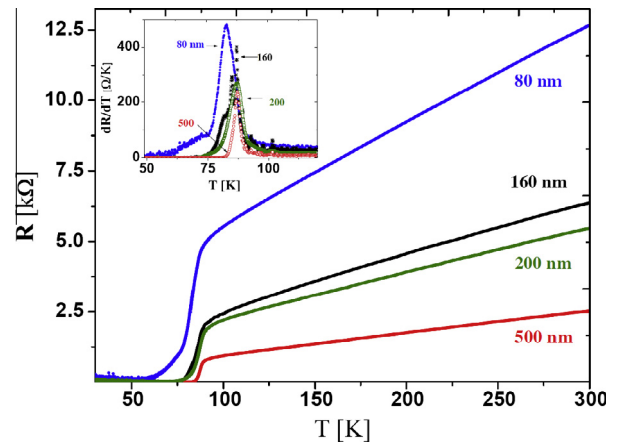


Fig. 2. Temperature dependence of the zero-field resistance of 80, 160, 200 and 500 nm YBCO bridges (blue, black, green and red lines, respectively), measured with bias current of 5 μA. The bridges are 700 nm long and 10 nm thick. Inset: temperature derivative of the resistance for the four bridges. (For interpretation of the references to colour in this figure legend, the reader is referred to the web version of this article.)

is not observable below a certain temperature. However, as the dimensions of the bridge are reduced the probability for such current-flow channels is decreased causing a transition broadening to lower temperatures.

3.2. *V*–*I* characteristics

V–*I* curves were measured in a different set of bridges, patterned on a 20 nm thick granular YBCO film. Typical curves are shown in Fig. 3, in a log–log scale, for a 500 × 700 nm² bridge. At low temperatures the log *V* vs. log *I* curves exhibit three regions with a maximum slope in the middle range. The knee defining the crossover to a maximum slope gradually disappears as temperature increases. One may attempt analyzing these data in the framework of the theory of Tafuri et al. [18] for thermally activated dissipation in ultra-thin superconducting bridges. This theory predicts a moderate increase of *V* with *I* at low currents crossing over to fast increasing power-law dependence, $V \propto I^n$. These two current regimes can be identified with the low and intermediate current regimes of the low temperatures *V*–*I* curves of Fig. 3. (The third, high current regime exhibits a smaller slope compared to the intermediate current regime, and hence cannot be analyzed in the framework of the above theory). The inset to Fig. 3 zooms at

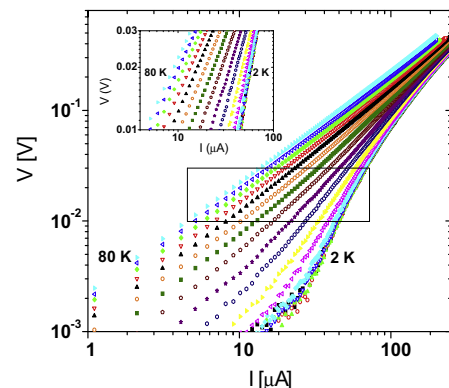


Fig. 3. Log–log plot of typical *V*–*I* curves in 20 × 500 × 700 nm³ YBCO bridge for temperatures between 2 and 80 K (with intervals of 5 K between 5 and 80 K). Inset: zoom on the intermediate current region, showing an approximate power-law behavior, $V \propto I^n$.

a range where a power law, $V-I^n$, is observed throughout the whole temperature range. In the terminology of Ref. [18] in this range $I > I_0$ at all temperatures. The temperature dependence of the power n extracted from the data in the inset to Fig. 3, is depicted in Fig. 4. As the figure shows, n saturates at low temperatures, in variance with the theoretically expected divergence of $n(T) = 1 + \Phi_0^2/8\pi^2 \lambda(T)kT$ for a thermally activated process. Here $\lambda = 2\lambda^2/d$ is the Pearl penetration length, λ the London penetration depth and d the bridge thickness. Similar behavior of $n(T)$ was previously observed by Tafuri et al. [18] in homogenous, 50–85 μm wide, ultra-thin high- T_c superconducting Ca–Cu–O sandwiched between Ba–Nd–Cu–O layers, and interpreted as a signature of quantum tunneling of Pearl vortices. To support their interpretation Tafuri et al. showed a linear dependence of $\ln(V)$ vs. I^{-2} , a behavior predicted for a quantum tunneling process. A plot of $\ln(V)$ vs. I^{-2} for our data (see inset to Fig. 4) fails to show this linear dependence, refuting the quantum-tunneling interpretation in our case [20].

The saturation in $n(T)$ at low temperatures and the high current behavior at low temperatures lead to an alternative explanation that takes into account the granular nature of our bridges. The YBCO bridge can be viewed as an array of Josephson junctions with a distribution of critical currents, I_c and normal resistances R_n . Assuming overdamped junctions, the voltage–current relationship for each junction is described by $V = R_n(I^2 - I_c^2)^{1/2}$ for $I > I_c$, whereas $V = 0$ for $I < I_c$. Voltage can be measured across the bridge only if the applied current exceeds the lower edge of the critical current distribution. A fast increase of the voltage (as observed in the intermediate region of the $V-I$ curves at low temperatures in Fig. 3) occurs at applied currents corresponding to critical currents in the central part of the I_c is distribution (each junction for which $I \gtrsim I_c$ contributes a sharp increase in V). Upon further increasing I , for the majority of the junctions $I > I_c$ and therefore the increase of V with I becomes more moderate (as observed in the third region of the low temperatures $V-I$ curve in Fig. 3), crossing over to a linear increase for I much larger than the largest critical currents in the distribution. The saturation of $n(T)$ at low temperatures is directly related to the saturation of the critical current distribution at these temperatures. It should be noted that according to this explanation the $V-I$ curve is not governed by thermally activated processes but rather by the critical current distribution of the Josephson junctions array.

It should be noted that some bridges exhibit jumps in the $V-I$ curves far below the transition temperature. This is demonstrated

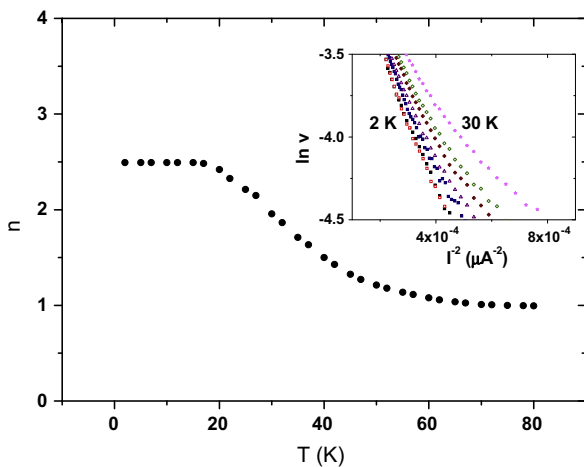


Fig. 4. Temperature dependence of the exponent n characterizing the power–lower behavior $V-I^n$ of the inset to Fig. 3. Inset: $\ln(V)$ vs. I^{-2} at 2, 10, 20, 22, 25, 27, and 30 K for the same voltage range as in the inset to Fig. 3.

in Fig. 5 for a $20 \times 200 \times 700 \text{ nm}^3$ bridge. The voltage V^* and the current I^* for which the jumps occur are plotted in the inset to Fig. 5 as a function of temperature. Similar jumps were previously observed in YBCO films near T_c [21,22] and interpreted as resulting from Larkin–Ovchinnikov (LO) instabilities [23,24]. Xiao et al. [25] observed voltage jumps in YBCO films even at temperatures far below T_c and interpreted them as resulting from “hot spots”, namely self-heating due to local high current density (for a review of the self-heating effect in superconductors see Ref. [26]). Apparently, the jumps described in Fig. 5 can also be interpreted as resulting from the same effect, as they are observed at temperatures below 50 K, far below T_c . Moreover, the temperature dependence of I^* at high temperatures ($T = 30\text{--}50 \text{ K}$) fits the theoretically predicted behavior for I^* caused by hot spots effect [26]:

$$I^* = (2hdw^2T_c/\rho_N)^{1/2} (1 - T/T_c)^{1/2},$$

where d and w are the bridge thickness and width, respectively, and h is the heat transfer coefficient. The fit (solid line in the inset to Fig. 5) yields $(2hdw^2T_c/\rho_N)^{1/2} = 780 \mu\text{A}$. Using $d = 20 \text{ nm}$, $w = 500 \text{ nm}$, $T_c = 83 \text{ K}$, $\rho_N = 1450 \mu\Omega \text{ cm}$, the derived heat transfer coefficient h is $680 \text{ W/cm}^2 \text{ K}$, reasonably compared with values found in the literature [25,27]. As mentioned above, voltage jumps are not observed in all the samples; however they are more likely to occur in narrow granular bridges.

3.3. Magnetoresistance

The magnetoresistance of the bridges exhibit complex behavior, shown in Fig. 5 for the $10 \times 200 \times 700 \text{ nm}^3$ bridge for temperatures 30–86 K and fields up to 5 T, using a bias current of $2 \mu\text{A}$. (The zero-field critical current of the relevant bridge, estimated from $V-I$ curves, is $\sim 2 \mu\text{A}$ at 70 K.) The figure shows magnetoresistance oscillations superimposed on a background exhibiting distinctive behavior at low and high temperatures. While at high temperatures the background increases monotonically with the field, the low temperature data exhibit a *negative* magnetoresistance slope, $dR/d|H|$, in a wide field range in the Tesla regime. Similar results, with the same bias current, were obtained in narrower samples except the 80 nm wide bridge for a reason to be explained below.

Negative magnetoresistance slope was observed in various low- and high- T_c systems and various models were proposed to explain this phenomenon [28–30]. A different model, which relates to

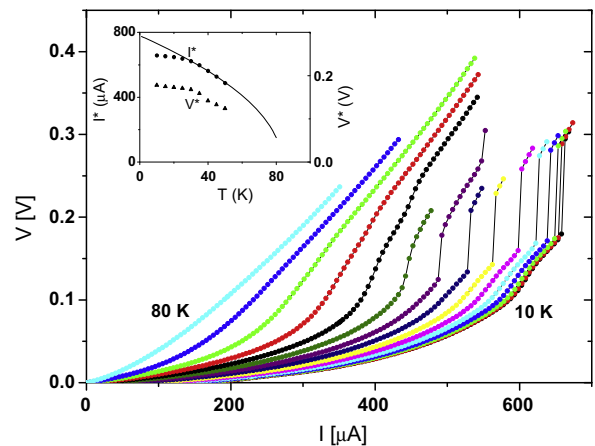


Fig. 5. $V-I$ curves in a $20 \times 200 \times 700 \text{ nm}^3$ YBCO bridge showing voltage jumps at current I^* and voltage V^* . Inset: temperature dependence of I^* and V^* . Solid line: fit of the high temperature data to the theoretical $I^*(T)$, see text.

granular materials, was described in Ref. [17]. In this model the complex magnetoresistance background observed in granular YBCO bridges is attributed to thermally activated phase slips in weak links and quasiparticles tunneling between grains. At high temperatures the first mechanism is dominant giving rise to an increase in the magnetoresistance due to enhanced phase slips rate with the field. Below a certain temperature the phase slips rate at high fields reaches saturation [31], giving rise to a constant magnetoresistance. In this temperature range the contribution of quasiparticles tunneling is revealed; as the field increases, more vortices enter the grains and the number of quasiparticles increases, enhancing conductivity by tunneling of quasiparticles [28] and hence exhibiting a negative magnetoresistance.

Theoretical calculations along similar lines were described in Ref. [32], viewing the granular system as a two-dimensional array of extended Josephson junctions. These calculations were based on the sine-Gordon equation describing the temporal and spatial dependence of the phase in the Josephson junctions. The equation was extended to include a viscosity term that increases linearly with the external field. The origin of this term is the increase in the number of quasiparticles because of the increase in the number of vortices as the field increases. Including such a term in the sine-Gordon equation yields a negative magnetoresistance slope setting in around a field which is determined by the geometry (the junction width) and, therefore, it is independent of temperature. This behavior characterizes the magnetoresistance at low temperature where the contribution of the Abrikosov vortices to the voltage may be neglected. Including this contribution may change the magnetoresistance slope to zero and even to positive values.

Experimentally, we found that the negative slope can be eliminated by increasing the bias current [17]. The increased current has a similar effect as increasing temperature; both enhance the phase slips rate in the weak links. As a result, the effect of tunneling of quasiparticles is less significant and hence unobservable. This explains the absence of the negative magnetoresistance slope in the narrow (80 nm) bridge; as the same current range was used to measure the magnetoresistance in all the bridges, the bias current density was the largest in the narrowest wire, enhancing the phase slips rate and thus generating a positive magnetoresistance slope which masks the negative contribution from quasiparticles tunneling.

Magnetoresistance oscillations shown in Fig. 6 were already observed in granular low- T_c superconductors and ascribed to phase coherent loops that are established far below T_c [33–35]. The inset

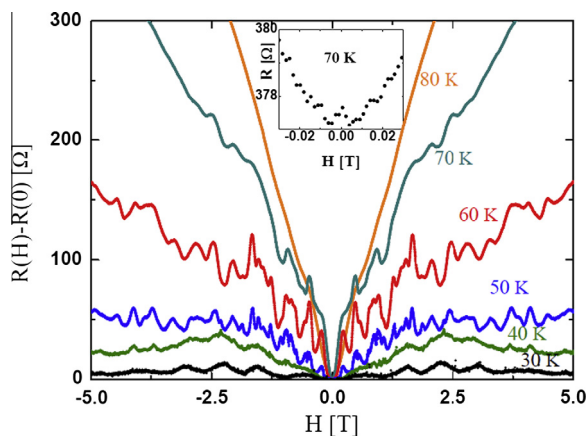


Fig. 6. Magnetoresistance isotherms between 30 and 80 K for the $10 \times 200 \times 700 \text{ nm}^3$ bridge, using a bias current of $2 \mu\text{A}$. All the magnetoresistance curves are shifted to zero at zero field by subtracting $R(0) = 11.5, 30.5, 106, 214, 378,$ and 965Ω from the 30, 40, 50, 60, 70, and 80 K data, respectively. Inset: zoom on the low-field limit of the 70 K data showing negative magnetoresistance around $H = 0$.

to Fig. 6 zooms at the 70 K magnetoresistance data near zero field, showing negative magnetoresistance, similar to that observed in low- T_c granular bridges [36–39]. This phenomenon was ascribed to various origins including pair scattering from magnetic impurities [40] and strong fluctuations near the superconducting-insulator transition (SIT) that induce a random distribution of negative and positive Josephson critical currents [41,42]. In Ref. [16] we argue that the negative magnetoresistance observed in granular YBCO is more likely to originate from Josephson π -junctions arising from the d-wave nature of the order parameter in this material.

4. Summary

Granular YBCO nano-bridges exhibit a rich spectrum of magneto-transport phenomena, including broadening of the transition region, negative magnetoresistance slope at high fields, negative magnetoresistance at low fields, magnetoresistance oscillations, V - I curves that exhibit temperature-independent power law at low temperatures and voltage jumps at temperatures well below T_c . All these phenomena are attributed to the granular nature of the bridges. Thus they may be manifested differently in different bridges even with the same dimensions, strongly depending on the starting film and the patterning process. All these factors should be taken into account in any future attempts to employ such bridges in electronic circuits and devices.

Acknowledgements

Valuable discussions with Rudolf Huebener and Vladimir Kogan are acknowledged. Y.Y. acknowledges a support of the Israel Science Foundation (Grant No. 164/12).

References

- [1] S. Anders, M.G. Blamire, F. Im Buchholz, D.G. Cr  t  , R. Cristiano, P. Febvre, L. Fritzsche, A. Herr, E. Il'ichev, J. Kohlmann, J. Kunert, H.G. Meyer, J. Niemeyer, T. Ortlev, H. Rogalla, T. Schurig, M. Siegel, R. Stolz, E. Tarte, H.J.M. ter Brake, H. Toepfer, J.C. Villegier, A.M. Zagorskin, A.B. Zorin, *Phys. C: Supercond.* 470 (2010) 2079.
- [2] K. Yu Arutyunov, D.S. Golubev, A.D. Zaikin, *Phys. Rep.* 464 (2008) 1.
- [3] E.A. Duarte, P.A. Quintero, M.W. Meisel, J.C. Nino, *Phys. C: Supercond.* 495 (2013) 109.
- [4] S.H. Lai, Y.C. Hsu, M.D. Lan, *Solid State Commun.* 148 (2008) 452.
- [5] F. Carillo, G.M. De Luca, D. Montemurro, G. Papari, M. Salluzzo, D. Stornaiuolo, F. Tafuri, F. Beltram, *New J. Phys.* 14 (2012) 025.
- [6] X.L. Lu, G.Q. Zhang, J.F. Qu, W. Wang, Y.Q. Zhang, X.G. Li, *Phys. C: Supercond.* 460–462 (2007) 1438, Part 2.
- [7] I. Sochnikov, A. Shaulov, Y. Yeshurun, G. Logvenov, I. Bozovic, *Nat. Nano* 5 (2010) 516.
- [8] D.H.A. Blank, W. Booij, H. Hilgenkamp, B. Vulink, D. Veldhuis, H. Rogalla, *Appl. Supercond. IEEE Trans.* 5 (1995) 2786.
- [9] N. Curtz, E. Koller, H. Zbinden, M. Decroux, L. Antognazza,  . Fischer, N. Gisin, *Supercond. Sci. Technol.* 23 (2010) 045015.
- [10] K. Xu, J.R. Heath, *Nano Lett.* 8 (2008) 3845.
- [11] G. Zhang, X. Lu, T. Zhang, J. Qu, W. Wang, X. Li, S. Yu, *Nanotechnology* 17 (2006) 4252.
- [12] H. Jiang, Y. Huang, H. How, S. Zhang, C. Vittoria, A. Widom, D.B. Chrisey, J.S. Horwitz, R. Lee, *Phys. Rev. Lett.* 66 (1991) 1785.
- [13] J.A. Bonetti, D.S. Caplan, D.J. Van Harlingen, M.B. Weissman, *Phys. Rev. Lett.* 93 (2004) 087002.
- [14] P. Mikheenko, X. Deng, S. Gildert, M.S. Colclough, R.A. Smith, C.M. Muirhead, P.D. Prewett, J. Teng, *Phys. Rev. B* 72 (2005) 174506.
- [15] R. Arpaia, S. Nawaz, F. Lombardi, T. Bauch, *Appl. Supercond. IEEE Trans.* 23 (2013) 1101505.
- [16] D. Levi, A. Shaulov, A. Frydman, G. Koren, B.Ya. Shapiro, Y. Yeshurun, *EPL Europhys. Lett.* 101 (2013) 67005.
- [17] D. Levi, A. Shaulov, G. Koren, Y. Yeshurun, *Phys. C: Supercond.* 495 (2013) 39.
- [18] F. Tafuri, J.R. Kirtley, D. Born, D. Stornaiuolo, P.G. Medaglia, P. Orgiani, G. Balestrino, V.G. Kogan, *EPL Europhys. Lett.* 73 (2006) 948.
- [19] G. Koren, A. Gupta, E.A. Giess, A. Segm  ller, R.B. Laibowitz, *Appl. Phys. Lett.* 54 (1989) 1054.
- [20] The nearly linear plot at 2–10 K may suggest a linear dependence at temperatures below 2 K.
- [21] S.G. Doettinger, R.P. Huebener, R. Gerdemann, A. K  hle, S. Anders, T.G. Tr  uble, J.C. Villegier, *Phys. Rev. Lett.* 73 (1994) 1691.

- [22] Z.L. Xiao, P. Ziemann, *Phys. Rev. B* 53 (1996) 15265.
- [23] A.I. Larkin, Y.N. Ovchinnikov, *Sov. Phys. – JETP Engl. Trans. United States* 46 (1) (1977) 155. Medium: X.
- [24] A.I. Larkin, Y.U.N. Ovchinnikov, *Sov. Phys. JETP* 41 (1975) 960.
- [25] Z.L. Xiao, E.Y. Andrei, P. Ziemann, *Phys. Rev. B* 58 (1998) 11185.
- [26] A.V. Gurevich, R.G. Mints, *Rev. Mod. Phys.* 59 (1987) 941.
- [27] M. Nahum, S. Verghese, P.L. Richards, K. Char, *Appl. Phys. Lett.* 59 (1991) 2034.
- [28] N. Morozov, L. Krusin-Elbaum, T. Shibauchi, L.N. Bulaevskii, M.P. Maley, Yu I. Latyshev, T. Yamashita, *Phys. Rev. Lett.* 84 (2000) 1784.
- [29] R. Córdoba, T.I. Baturina, J. Sesé, A. Yu Mironov, J.M. De Teresa, M.R. Ibarra, D.A. Nasimov, A.K. Gutakovskii, A.V. Latyshev, I. Guillamón, H. Suderow, S. Vieira, M.R. Baklanov, J.J. Palacios, V.M. Vinokur, *Nat. Commun.* 4 (2013) 1437.
- [30] H. Jeffrey Gardner, Ashwani Kumar, Liuqi Yu, Peng Xiong, Maitri P. Warusawithana, Luyang Wang, Oskar Vafeek, Darrell G. Schlom, *Nat. Phys.* 7 (2011) 895.
- [31] M. Tinkham, *Phys. Rev. Lett.* 61 (1988) 1658.
- [32] B.Ya. Shapiro, I. Shapiro, D. Levi, A. Shaulov, Y. Yeshurun, *Physica C* (2014).
- [33] A.V. Herzog, P. Xiong, R.C. Dynes, *Phys. Rev. B* 58 (1998) 14199.
- [34] A. Johansson, G. Sambandamurthy, D. Shahar, N. Jacobson, R. Tenne, *Phys. Rev. Lett.* 95 (2005) 116805.
- [35] U. Patel, Z.L. Xiao, A. Gurevich, S. Avci, J. Hua, R. Divan, U. Welp, W.K. Kwok, *Phys. Rev. B* 80 (2009) 012504.
- [36] P. Xiong, A.V. Herzog, R.C. Dynes, *Phys. Rev. Lett.* 78 (1997) 927.
- [37] P. Santhanam, C.C. Chi, S.J. Wind, M.J. Brady, J.J. Bucchignano, *Phys. Rev. Lett.* 66 (1991) 2254.
- [38] Y.K. Kwong, K. Lin, P.J. Hakonen, M.S. Isaacson, J.M. Parpia, *Phys. Rev. B* 44 (1991) 462.
- [39] P. Santhanam, C.P. Umbach, C.C. Chi, *Phys. Rev. B* 40 (1989) 11392.
- [40] Y.B. Simons, O. Entin-Wohlman, Y. Oreg, Y. Imry, *Phys. Rev. B* 86 (2012) 064509.
- [41] S.A. Kivelson, B.Z. Spivak, *Phys. Rev. B* 45 (1992) 10490.
- [42] B.I. Spivak, S.A. Kivelson, *Phys. Rev. B* 43 (1991) 3740.